Article

Qualitative Analysis of Nitrogen and Sulfur Compounds in Vacuum Gas Oils via Matrix-Assisted Laser Desorption Ionization Time of Flight Mass Spectrometry

Morio Ueda [1], Jongbeom Lee [2], Hyeonseok Yi [3], Gang-Ho Lee [3], Yu-Jin Kim [2], Geon-Hee Kim [4], Kyeongseok Oh [5], Seong-Ho Yoon [6], Koji Nakabayashi [6,*] and Joo-Il Park [2,*]

[1] Kyushu Environmental Evaluation Association, Fukuoka 813-0004, Japan
[2] Department of Chemical & Biological Engineering, Hanbat National University, Daejeon 34158, Republic of Korea
[3] Carbon Materials Research Group, Research Institute of Industrial Science & Technology (RIST), Pohang 37673, Republic of Korea; h.yi@rist.re.kr (H.Y.)
[4] Department of Defense Space Engineering, Hanbat National University, Daejeon 34158, Republic of Korea
[5] Department of Chemical and Biological Engineering, Inha Technical College, Incheon 22212, Republic of Korea; kyeongseok.oh@inhatc.ac.kr
[6] Interdisciplinary Graduate School of Engineering Sciences, Kyushu University, Fukuoka 816-8580, Japan
[*] Correspondence: nakabayashi@cm.kyushu-u.ac.jp (K.N.); jipark94@hanbat.ac.kr (J.-I.P.);
    Fax: +81-92-583-7897 (K.N.); +82-42-821-1530 (J.-I.P.)

Abstract: Analysis of the heavy fractions in crude oil has been important in petroleum industries. It is well known that heavy fractions such as vacuum gas oils (VGOs) include heteroatoms, of which sulfur and nitrogen are often characterized in many cases. We conducted research regarding the molecular species analysis of VGOs. Further refine processes using VGOs are becoming important when considering carbon recycling. In this work, we attempted to classify compounds within VGOs provided by Kuwait Institute for Scientific Research. Two VGOs were priorly distilled from Kuwait Export crude and Lower Fars crude. Quantitative analysis was performed mainly using matrix-assisted laser desorption ionization time of flight mass spectrometry (MALDI-TOFMS). MALDI-TOF-MS has been developed for analyzing high-molecular-weight compounds such as polymer and biopolymers. As matrix selection is one of the most important aspects in MALDI-TOFMS, the careful selection of a matrix was firstly evaluated, followed by analysis using a Kendrick plot with nominal mass series (z^*). The objective was to evaluate if this work could provide an effective classification of VGOs compounds. The Kendrick plot is a well-known method for processing mass data. The difference in the Kendrick mass defect (KMD) between $C_nH_{2n-14}S$ and $C_nH_{2n-20}O$ is only 0.0005 mass units, which makes it difficult in general to distinguish these compounds. However, since the z^* value showed effective differences during the classification of these compounds, qualitative analysis could be possible. The analysis using nominal mass series showed the potential to be used as an effective method in analyzing heavy fractions.

Keywords: atmospheric residue; heavy oil; atmospheric residue desulfurization; molecular characterization; FT-ICR MS

1. Introduction

The demand for light distillates is increasing rapidly due to the growth of the population worldwide. Vacuum gas oil (VGO) is an intermediate fraction from crude oil and serves as an important source of catalytic cracking and hydrocracking [1–3]. VGO, known as a heavy distillate, shows difficulties during the cracking process because of the existence of its intrinsic heteroatoms, such as sulfur and nitrogen. High capital costs are needed when a new unit process is considered for treating VGO. Nevertheless, global interest in the production of ultra-low-sulfur fuels has grown significantly. Sulfur compounds in

liquid fuels generate sulfur oxides and other pollutants during combustion, which later cause acid rain and other types of environmental pollution. Since it is important to design the facilities for removing sulfur-containing compounds in liquid hydrocarbon fuels, the characterization of heavy oil can be essential for the conversion of heavy fractions into low-boiling-point fractions. Until recently, low-boiling-point fractions such as atmospheric gas oil have been analyzed in detail using capillary gas chromatography (GC) [4–9]. However, owing to the low volatility of high-molecular-weight compounds, it is difficult to analyze heavier distillates via GC. Fourier transform ion cyclotron resonance mass spectrometry (FTICR-MS) is often used for analyzing heavier materials and can clarify the structure of high-boiling-point fractions [10–27]. FTICR-MS is a powerful method for analyzing heavy oils, such as atmospheric residue, vacuum residue and asphaltene. Meanwhile, conventional analyses for VGO compounds using 1D and/or 2D GC mass spectrometry (GC-MS) [28–30] have been reported. Chen et al. [12] reported that six basic nitrogen compounds, N_1 (a molecule containing one nitrogen atom), N_1O_1, $N_1O_1S_1$, N_1O_2, N_1S_1 and N_2, were identified using positive-ion mass spectra, while non-basic nitrogen compounds, N_1, N_1O_1, N_1S_1 and N_2, are characterized by negative-ion mass spectra. Among these nitrogen compounds, N_1-class species are predominant. FTICR-MS data indicated that the basic N_1 class species are pyridines, quinolines and benzoquinolines, and most non-basic N_1 class species are derivatives of benzocarbazoles. Schaub et al. [11] reported that favorable core structures were identified as monosulfur compounds (e.g., thiophenes, benzothiophenes and dibenzothiophenes). The most abundant S_1 class species seems to be benzothiophenes and dibenzothiophenes. Even though FTICR-MS showed effectiveness in a detailed speciation of a heavy fraction, the equipment's installation and operation costs were highly expensive.

In this work, we attempted to classify compounds in VGOs via matrix-assisted laser desorption ionization time of flight mass spectrometry (MALDI-TOF-MS). The MALDI-TOF method disperses the target sample uniformly in a matrix that absorbs the wavelength of an ultraviolet laser (nitrogen laser light: 337 nm) and irradiates the laser. When the laser irradiates the matrix, the laser light is converted into thermal energy. At this time, the matrix is rapidly heated and vaporized, and at the same time, the sample surrounded by the matrix also receives energy from the matrix and vaporizes. This ionizes, accelerates and detects the sample in the TOF/MS electric field space. The TOF/MS analyzer offers high sensitivity and selectivity for wide-range screening. It provides accurate measurement of ionizable component mass with few mass errors. This technique is ideal for both non-target and post-target analysis. Since the sample is ionized via the matrix, it is possible to measure a sample (protein, etc.) that is sensitive to heat and easily decomposed without causing fragmentation. This method can measure up to the highest-mass region compared with the mass spectrometry methods currently used, and can measure the molecular weight distribution and perform structural analysis at the same time and in a short time [31]. Although many scientists have identified compounds using both MALDI-TOF-MS and FTICR-MS [32,33], this work explores the sole employment of MALDI-TOF-MS, mainly to identify sulfur compounds and nitrogen compounds. It may bring up a fundamental question: is it possible to classify and identify compounds using MALDI-TOF-MS only? In general, it is difficult to analyze low-molecular-weight compounds with MALDI-TOF-MS, unlike the case for analyzing high-molecular-weight compounds. As reported, matrix selection is one of the most important aspects of MALDI-TOF-MS. This work proposes the classification of compounds in VGO feeds as well as hydrodesulfurization-treated VGOs by selecting the appropriate matrix. The analytical procedure was performed after pretreating samples. The Kendrick mass plot was employed to analyze sulfur and nitrogen in detail.

2. Experimental

2.1. VGO Feeds and Their HDS Reaction

Two different VGOs were used as received from the Kuwait Institute for Scientific Research. Two VGO samples were obtained from Kuwait Export crude and Lower Fars

crude, named KEC-VGO and LFC-VGO, respectively. The boiling points of KEC-VGO and LFC-VGO were 350–538 °C and 350–523 °C, respectively. In case of HDS products, two VGOs were treated in a 150 mL batch autoclave (RX Engineering Co. Ltd., Anyang-si, Republic of Korea), equipped with a magnetic stirrer rotating at 300 rpm in the laboratory. Each 30 g VGO feed was treated at 370 °C for 0.5 h under an initial H_2 pressure of 9 Mpa in the presence of 3 g of $CoMo/Al_2O_3$ catalyst. The catalyst was supplied by ART Corporation (Kawasaki, Japan).

2.2. Solvent Fractionation

Sulfur and nitrogen compounds in both VGOs and their HDS products were fractionated according to an established procedure [1]. The fractionation procedure is shown in Figure 1 [34]. Activated neutral alumina (80 g) was dried at 180 °C for 4 h under vacuum conditions and then packed into a glass column (30 mm i.d. and 600 mm long). Each VGO (approximately 10 g) was placed on the top of the column. The extraction sample was eluted first with 100 mL of n-hexane for the saturated hydrocarbon fraction, and with 100 mL of n-hexane/dichloromethane (60/40 *v/v*) for the aromatic and sulfur compound fractions. The nitrogen compound and polar fraction were eluted by 200 mL of dichloromethane and 200 mL of methanol, respectively. The solvent of each fraction was evaporated under vacuum conditions, and the saturated hydrocarbon fraction and aromatic and sulfur compound fractions were collected using a Pasteur pipet. The nitrogen fraction and polar fraction were dissolved by tetrahydrofuran (THF) and collected.
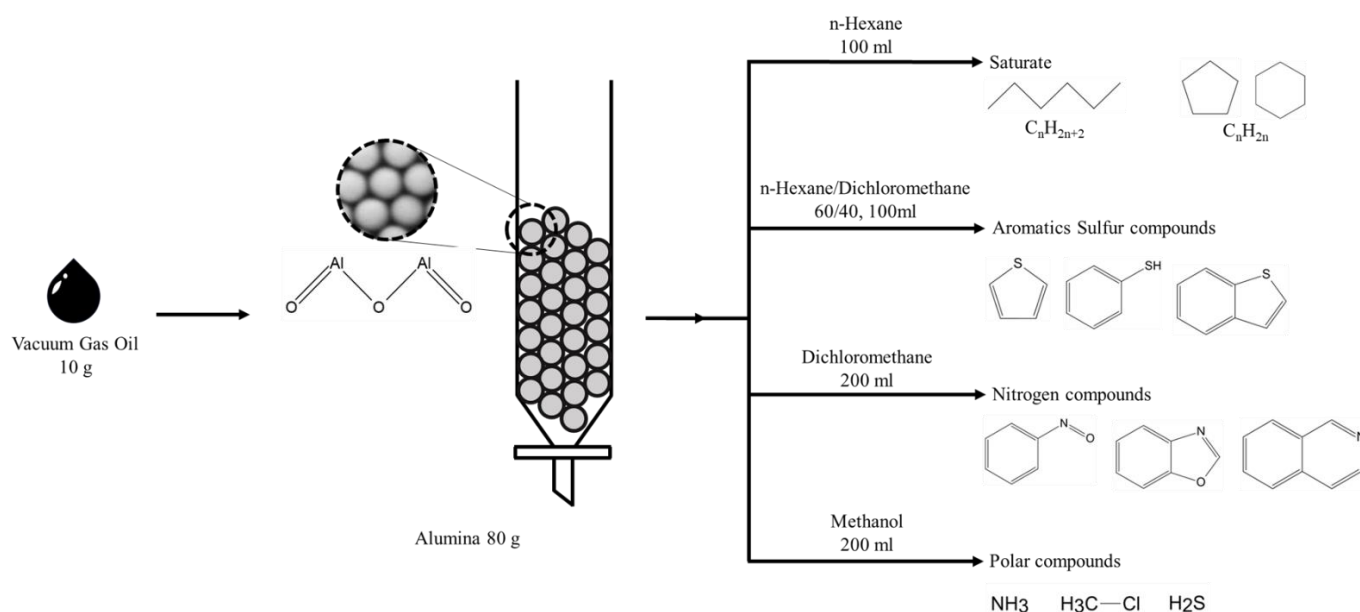

Figure 1. Separation method for VGO.

In the MALDI-TOF-MS analysis, a number of peaks were noted after sample separation, whereas there were no clear peaks in the non-separated sample. When many compounds are present in a sample, it is possible that one of them will prevent the others from being ionized, while another compound could facilitate the ionization of the others, according to a matrix-like effect. Since a crude oil consists of many compounds, it is not easy task to determine each compound's individual effect on ionization. However, based on the appearance of peaks after separation, it is hypothesized that some compounds prevent the ionization of other compounds, as alluded to previously. In this work, separating the feed into fractions was a useful method.

2.3. Sample Preparation for MALDI-TOF-MS

In the previous study, TCNQ (2 7,7,8,8-tetracyanoquinodimethane) was introduced as the optimal matrix for the analysis of heavy fractions in MALDI-TOF-MS [35]. In this work, to verify the effectiveness of TCNQ, 4,6-dimethyldibenzothiophene was evaluated using TCNQ and α-cyano-4-hydroxycinnamic acid (CHCA). The chemical structures of both matrix chemicals are presented in Figure 2. TCNQ performs as an electron acceptor because it has four cyano groups, and tends to promote radical compounds. On the other hand, CHCA has one cyano group, one hydroxyl group and one carboxyl group, such that CHCA renders compounds not only radical, but also protonated. Thus, the ionized conditions of peaks obtained by this matrix are difficult to interpret sufficiently (Figure 3). Figure 4 shows the detected peaks. An amount of 10 g of each fraction of VGO feeds and their HDS products were dissolved in 1 mL of THF, and 10 mg of TCNQ was also dissolved in 1 mL of THF. Oil fractions were also mixed with some standard samples. The samples and matrix in THF were mixed in a 1:1 (*v*/*v*) ratio, and then 1 μL of the mixture was spotted on the sample plate. The fraction and nitrogen fraction amounts were quite small, so these fractions were dissolved in THF and collected after separation; then, the THF solutions were also mixed with standard samples and a matrix solvent in a 1:1 ratio. To obtain high-resolution data, external and internal standards (Table 1) were used. Carbazole, anthracene, 4,6-dimethyldibenzothiophene (4,6-DMDBT), pyrene, benzonaphthothiophene (BNT), perylene, coronene, dibenzochrysene (DBC) and dibenzopentacene (DBP) polyethyleneglycol (PEG) were chosen as external standards. The mixing ratio of these compounds was 40:15:100:15:10:1:5:4:5:1.5 (wt.%) [35] In addition, anthracene 4,6-DMDBT, perylene, coronene, benzocarbazole, DBC and PEG were used as internal standards. The chemical structures of the external and internal standards are presented in Table 2. Each internal standard sample amount of 1 or 10 mg was dissolved in THF. For example, a 10 μL polar fraction solution of KEC-VGO was mixed with 1 μL of coronene solution (1 mg/mL), and this mixture was in turn mixed with TCNQ solution in a 1:1 ratio and spotted on the sample plate. The mixing ratios of each fraction used in this study are shown in Table 2. Samples were analyzed using MALDI-TOF-MS (JMS-S3000; Japan Electron Optics Laboratory, Tokyo, Japan). In the polar fraction of KEC-VGO, high-resolution data were obtained from external and internal standard samples. For example, the theoretical mass values of benzocarbazoles, benzoacridines, dibenzocarbazoles and tetrahydrodibenzoacridines are 273.15120, 285.15120, 295.13555 and 297.15120, and the mass values measured using the external and internal standard methods are 273.15128, 285.15112, 295.13563 and 297.15122, respectively.
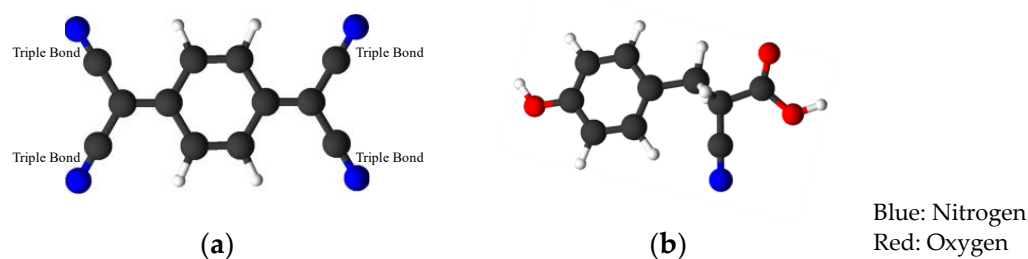

Blue: Nitrogen
Red: Oxygen

(**a**)   (**b**)

Figure 2. Matrix chemical structures of (**a**) 7,7,8,8,-tetracyanoquinodimethane (TCNQ) and (**b**) α-cyano-4-hydroxycinnamic acid.
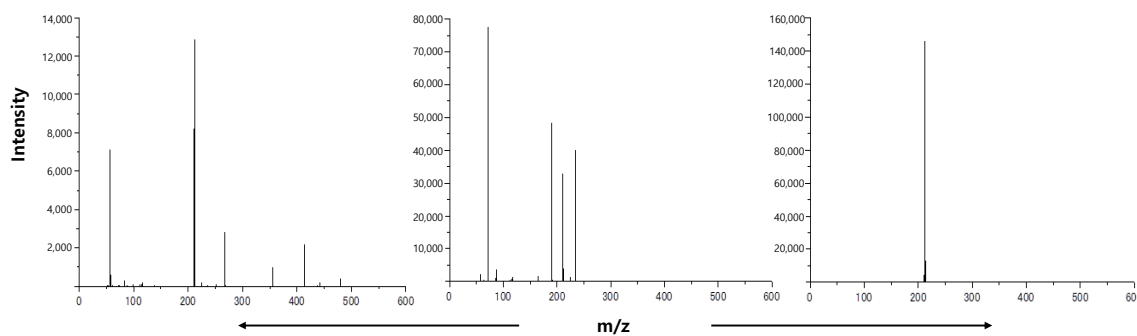
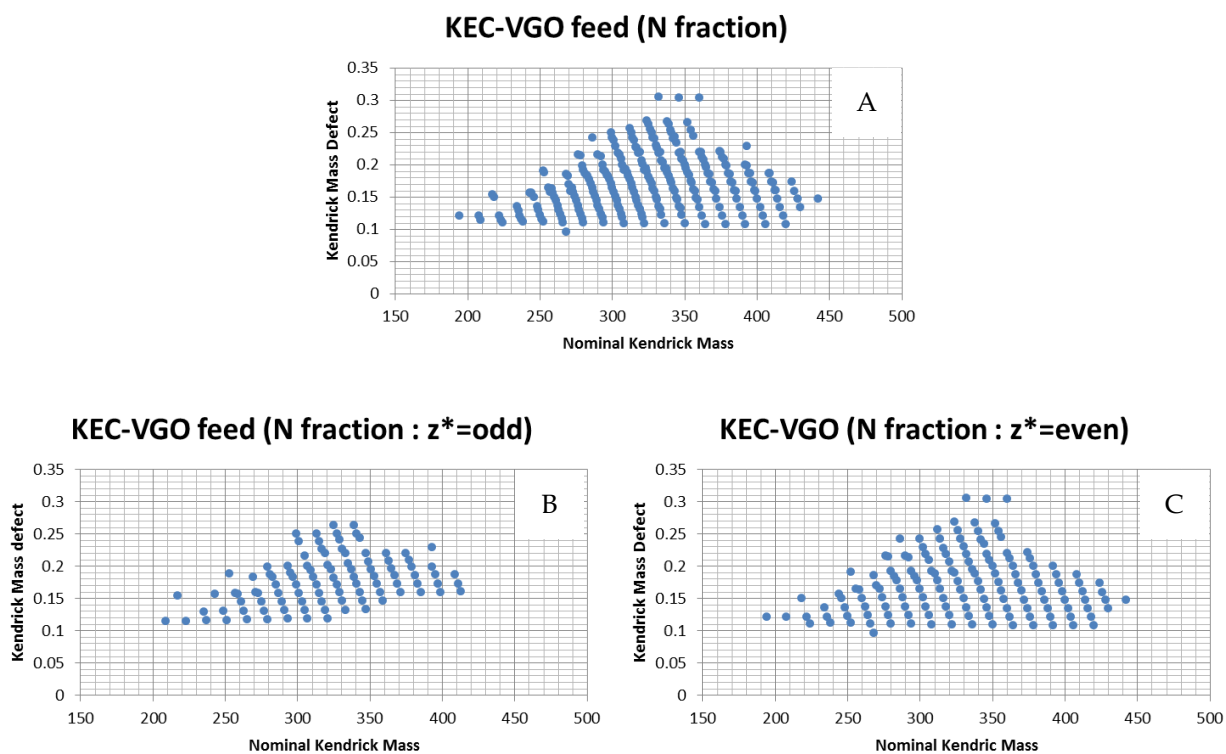**Figure 3.** Peaks of 4,6-dimethyldibenzothiophene (**left**: without matrix; **center**: with CHCA; **right**: TCNQ).

Figure 4. Kendrick plot of KEC-VGO feed before and after pre-sorting (**A**: without pre-sorting; **B**: z* = odd; **C**: z* = even).

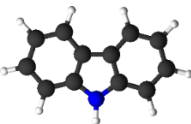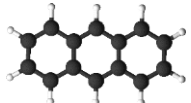**Table 1.** Chemical structures of external and internal standards.

Name	Structure	External	Internal
Carbazole	Blue: Nitrogen	O	
Anthracene		O	O

Table 1. *Cont.*
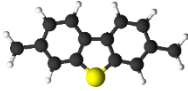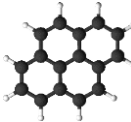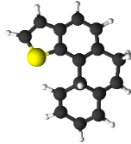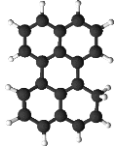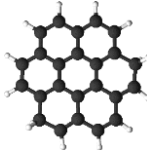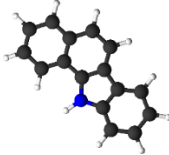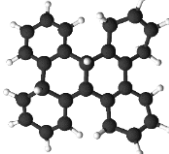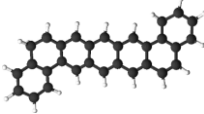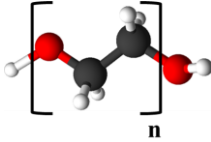
Name	Structure	External	Internal
4,6-dimethyldibenzothiophene (4,6-DMDBT)	Yellow: Sulfur	O	O
Pyrene		O	
benzonaphthothiophene	Yellow: Sulfur	O	
Perylene		O	O
coronene		O	O
benzocarbazole	Blue: Nitrogen		O
Dibenzo[g,p]chrysene (DBC)		O	O
Dibenzo[a,l]pentacene (DBP)		O	
Polyethylene glycol (PEG)	Red: Oxygen	O	O

Table 2. Mixing ratio of each fraction and internal standard samples.

	Fraction and Volume	Anthracene	4,6-DMDBT	Benzocarbazole	Perylene	Coronene	DBC	PEG
KEC-VGO feed	Polar 10 µL	-	-	-	-	1 µL (1 mg/mL)	-	-
	Nitrogen 10 µL	-	-	10 µL (1 mg/mL)	1 µL (1 mg/mL)		1 µL (1 mg/mL)	3 µL (10 mg/mL)
	Aromatics + Sulfur 10 µL (10 mg)	-	-	1 µL (1 mg/mL)	-	-	1 µL (1 mg/mL)	1 µL (10 mg/mL)
KEC-VGO HDS products	Polar 1000 µL	-	100 µL (1 mg/mL)	-	-	0.3 µL (1 mg/mL)	-	
	Nitrogen 10 µL	-	5 µL (1 mg/mL)	-	-	-	1 µL (1 mg/mL)	1 µL (10 mg/mL)
	Aromatics + Sulfur 100 µL (100 mg)	1 µL (1 mg/mL)	-	-	-	1 µL (1 mg/mL)	1 µL (10 mg/mL)	
LFC-VGO feed	Polar 10 µL	-	-	-	1 µL (1 mg/mL)	-	-	-
	Nitrogen 10 µL	-	-	10 µL (1 mg/mL)	-	-	3 µL (1 mg/mL)	3 µL (10 mg/mL)
	Aromatics + Sulfur 10 µL (10 mg/mL)	1 µL (1 mg/mL)	-	-	-	-	1 µL (1 mg/mL)	1 µL (10 mg/mL)
LFC-VGO HDS products	Polar 1000 µL	-	100 µL (1 mg/mL)	-	-	0.3 µL (1 mg/mL)	-	-
	Nitrogen 10 µL	-	10 µL (1 mg/mL)	-	-	-	1 µL (1 mg/mL)	-
	Aromatics + Sulfur 100 µL (10 mg/mL)	-	50 µL (10 mg/mL)	-	-	0.5 µL (1 mg/mL)	0.1 µL (10 mg/mL)	-

2.4. Kendrick Plot and Nominal Mass Series (z*)

It is known that numerous isomers make it difficult to identify each molecular species in the heavy fraction. The Kendrick plot was proposed to analyze heavy fractions, and formed the basis of the Kendrick mass defect (KMD) plot, where the KMD can be plotted against the nominal Kendrick mass (NKM) [36]. The advantage of the Kendrick plot is that members of a homologous series have identical KMD values, and the KMD has a positive correlation with the double-bond equivalent (DBE). The KMD plots are generated by multiplying the m/z of MALDI-TOF-MS data by 14.00000 and dividing the result by 14.01565, while the NKM is obtained by rounding the Kendrick mass value to the nearest integer:

$$\text{Kendrick mass} = m/z \times 14.00000/14.01565$$

Nominal Kendrick mass (NKM) = the nearest integer to the Kendrick mass value

The KMD can be obtained as follows:

$$\text{Kendrick mass defect} = \text{NKM} - \text{Kendrick mass}$$

To process high-resolution mass spectral data, a multiple sorting technique based on nominal mass series (z*) is effective, as is KMD [5]. The difference in KMD between $C_nH_{2n-14}S$ and $C_nH_{2n-20}O$ is only 0.0005 mass units. Therefore, it is not easy to distinguish between oxygen compounds and sulfur compounds, but the z* for $C_nH_{2n-14}S$ and $C_nH_{2n-20}O$ is −10 and −4, respectively, where z* is defined as follows:

$$z^* = \text{the modulus of (nominal mass/14)} - 14$$

The z* value is between -14 and -1 and is related to the valence number of the heteroatom. For example, the valence number of a sulfur atom is 2, so the z* of S-containing compounds is even. On the other hand, the z* of N-containing compounds is odd because the valence number of a nitrogen atom is 3. However, in the case of a compound with one sulfur atom and one nitrogen atom (S_1N_1 class species), the z* is odd because the total valence number is odd. In other words, compounds with odd z* values are N_1, N_1S_1, N_1O_1, $N_1S_1O_1$, N_1S_2, $N_1 O_2$, N_3 and so on, while S_1, O_1, S_2, O_2, S_1O_1, N_2, N_2S_1 and N_2O_1 have even z* values. The z* values are well separated to distinguish between compounds with similar KMDs. Kendrick plots can be relatively complicated due to the presence of many compounds in oil, but clarity can be achieved by pre-sorting (Figure 3). Thus, masses were sorted according to the z* value before KMD sorting. In this study, z* = odd for polar and nitrogen fractions, and even for aromatic and sulfur fractions.

2.5. GPC-UV Measurement

GPC-UV analysis was performed using a 1200 infinity series GPC instrument (Agilent technologies, Santa Clara, CA, USA) equipped with Diode Array Detector (DAD at 261 nm), an injection valve with a 300 μL loop. An LF-404 column (4.6 mm $\times$ 250 mm, Shodex, Tokyo, Japan) with 6 μm particle size 'multi-pore' gel as the stationary phase was used for high-resolution spectroscopy, and the LF-G column (4.6 mm $\times$ 10 mm, Shodex, Japan) was used as a guard column. Polystyrene commercial standard samples (SL-105, Shodex, Japan) were used for calibration. The mobile phase was THF in order to enhance the solubility of oil samples. Each standard sample was prepared by diluting a nominal concentration of 0.1% in THF and filtered by using a membrane filter (0.45 μm, Teflon, Millipore, St. Louis, MO, USA) in this study. The oil samples were also dissolved and filtered. The column temperature was stabilized at 40 °C. The THF solvent flowed overnight for stabilization. The flow rate was fixed at 0.2 mL min^{-1}, and a 5 μL aliquot of the oil sample was analyzed.

3. Results and Discussions

3.1. Classification of Compounds in KEC-VGO Feed and HDS Products

3.1.1. Polar and Nitrogen Fraction in KEC-VGO Feed and HDS Products

As mentioned in the experimental section, pre-z* sorting can be an effective method to classify the type of compounds present. The m/z of each fraction in KEC-VGO was determined based on the z* number and plotted on a Kendrick plot (Figure 5). In the case of odd z* values, many N_1 species were classified. In particular, in the polar and nitrogen fraction, N_1 class species were dominant and few S_1N_1 class species were present (Table 3). N_1 class species are expected to have a carbazole or acridine structure. Based on the KMD plot, $C_nH_{2n-15}N$, $C_nH_{2n-17}N$, $C_nH_{2n-19}N$, $C_nH_{2n-21}N$, $C_nH_{2n-23}N$, $C_nH_{2n-25}N$ and $C_nH_{2n-27}N$ are carbazole, acridine, tetrahydrobenzoacridine, benzocarbazole, benzoacridine, tetrahydrodibenzoacridine and dibenzocarbazole, respectively. N_1 class species were confirmed in the z* = odd polar and nitrogen fraction group, and the states of these compounds may be radical. Carbazoles and acridines have some benzene rings, so even if an electron in the pie orbital is removed, carbazoles and acridines in a radical state should be stable due to the delocalization of pie electrons. The function of the TCNQ matrix is to achieve a radical state, but not all of the compounds change into a radical state; some are protonated or become anions. N-containing compounds could be protonated. Because the nitrogen atom is a Lewis base, a proton can interact with the nitrogen atom in N-containing compounds. Thus, in the case of compounds with an N atom, not only is a radical structure detected, but so too is a protonated structure. If a proton is added to N-containing species, the z* value changes. For example, the z* value of radical benzoacridines is -9, but that of protonated benzoacridines is -8. Thus, in the polar and nitrogen fractions, nitrogen species could be detected in the even z* group, but it is possible to separate protonated compounds according to the pre-z* sorting step.
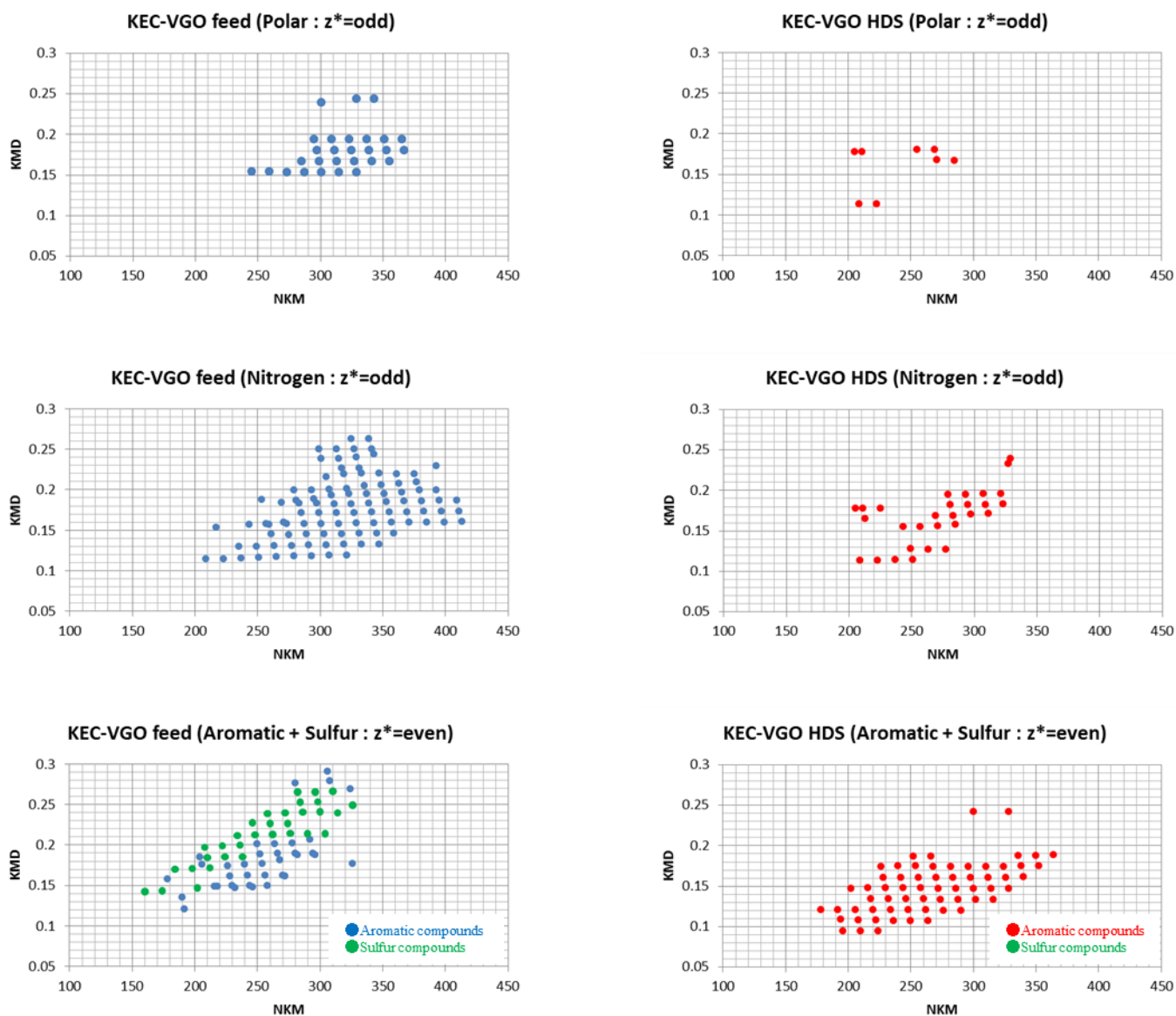
Figure 5. Kendrick plot of each fraction in KEC-VGO feed and HDS product.

Table 3. Expected structure of polar, nitrogen and aromatic + sulfur fraction in the KEC-VGO feed and HDS products. DBE represents the double bond equivalent.

| | | KEC-VGO | | |
Fraction	Formula (DBE)	Expected Structure	Feed	HDS Products
Polar	$CnH_{2n-25}SN$ (14)	-	O	
	$CnH_{2n-27}N$ (15)	Dibenzocarbazole	O	
	$CnH_{2n-25}N$ (14)	Tetrahydrodibenzoacridine	O	O
	$CnH_{2n-23}N$ (13)	Benzoacridine	O	O
	$CnH_{2n-21}N$ (12)	Benzocarbazole	O	
	$CnH_{2n-15}N$ (9)	Carbazole		O

Table 3. *Cont.*

Fraction	Formula (DBE)	KEC-VGO Expected Structure	Feed	HDS Products
Nitrogen	CnH2n-25SN (14)	-	O	
	CnH2n-23SN (13)	-	O	
	CnH2n-21SN (12)	-	O	
	CnH2n-19SN (11)	-	O	
	CnH2n-27N (15)	Dibenzocarbazole	O	
	CnH2n-25N (14)	Tetrahydrodibenzoacridine	O	
	CnH2n-23N (13)	Benzoacridine	O	
	CnH2n-21N (12)	Benzocarbazole	O	
	CnH2n-19N (11)	Tetrahydrobenzoacridine	O	
	CnH2n-17N (10)	Acridine	O	O
	CnH2n-15N (9)	Carbazole	O	O
Aromatic + Sulfur	CnH2n-30S (15)	Cholanthrenthiophene	O	
	CnH2n-28S (14)	Chrysenothiophene	O	
	CnH2n-26S (13)	Pyrenothiophene	O	
	CnH2n-24S (12)	Naphthenephenanthrenothiophene	O	
	CnH2n-30 (16)	Dicyclopentapyrene	O	
	CnH2n-20S (11)	Benzonaphthothiophene	O	
	CnH2n-28 (15)	Perylene	O	
	CnH2n-18S (10)	Acenaphthenothiophene	O	
	CnH2n-26 (14)	Tetrahydropicene	O	O
	CnH2n-16S (9)	Dibenzothiophene	O	
	CnH2n-24 (13)	Chrysene		O
	CnH2n-22 (12)	Pyrene	O	O
	CnH2n-12S (7)	Tetrahydrodibenzothiphene	O	
	CnH2n-20 (11)	Tetrahydrobenzoanthracene		O
	CnH2n-18 (10)	Anthracene	O	O
	CnH2n-16 (9)	Octahydronaphthacene		O

After the HDS reaction, the values of KMD decreased in both fractions, with compounds of a larger molecular weight being particularly affected. This shows that compounds of a high DBE are hydrogenated into products of a low DBE, and the molecular size of long alkyl chains of compounds is reduced. In the nitrogen fraction, after the HDS reaction, acridines and carbazoles were detected, and some compounds were confirmed within the 0.15 to 0.2 KMD range, but could not be classified.

3.1.2. Aromatic and Sulfur Fraction in KEC-VGO Feed and HDS Products

Several aromatic compounds and sulfur-containing compounds were confirmed in the aromatic and sulfur fractions. In the plot of aromatic and sulfur fractions, the KMD of sulfur compounds is larger than that of aromatics compounds. The formulas of the sulfur compounds are $C_nH_{2n-12}S$, $C_nH_{2n-16}S$, $C_nH_{2n-18}S$, $C_nH_{2n-20}S$, $C_nH_{2n-24}S$, $C_nH_{2n-26}S$, $C_nH_{2n-28}S$ and $C_nH_{2n-30}S$, and the structures corresponding to these formulas are tetrahydrodibenzothiophene, dibenzothiophene, acenaphthenothiophene, acenaphthlemothiophene, naphthenephenanthrenothiophene, pyrenothiophene, chrysenothiophene and cholanthrenthiophene, respectively. Aromatic compounds were confirmed in a small KMD area; the formulas are C_nH_{2n-16}, C_nH_{2n-18}, C_nH_{2n-20}, C_nH_{2n-22}, C_nH_{2n-24}, C_nH_{2n-26}, C_nH_{2n-28} and C_nH_{2n-30}, corresponding to octahydronaphthacene anthracene, tetrahydrobenzoanthracene, pyrene, chrysene, tetrahydropicene, perylene and dicyclopentapyrene, respectively. After the HDS reaction, a number of sulfur-containing compounds were reduced and peaks of aromatic compounds with small KMDs appeared. This result means that under hydrogen pressure, hydrogenation occurs alongside the HDS reaction on the CoMo catalyst. Interestingly, the molecular weight of some compounds in the HDS product was larger than that of some compounds in the feed.

3.2. Classification of Compounds in LFC-VGO Feed and HDS Products

3.2.1. Polar and Nitrogen Fraction in LFC-VGO Feed and HDS Products

As mentioned in the experimental section, pre-z* sorting is an effective method to classify the type of compounds present. The m/z of each fraction in LFC-VGO was determined based on the z* number and plotted on a Kendrick plot (Figure 6). As well as KEC-VGOs, some N_1 species were confirmed in the polar fraction of LFC-VGO, and the types of compounds were similar. However, S_1N_1 species could not be confirmed in the polar fraction in LFC-VGOs (Table 3). There were fewer peaks for the polar fraction of LFC-VGOs compared with that of KEC-VGOs, and the carbon number of the alkyl chains was small. After the HDS reaction, benzoacridines were present, but no other compounds were classified. In the nitrogen fraction, N_1 species were also dominant in the LFC-VGO feed, but there were fewer high-DBE species relative to the KEC-VGOs. Species with a high DBE were converted into compounds with a low DBE after the HDS reaction, and carbazoles, acridines, tetrahydrobenzoacridines, benzocarbazoles, benzoacridines and tetrahydrodibenzoacridines were detected. In particular, acridines and carbazoles in the HDS product of the LFC-VGOs had long alkyl chains compared with those of the HDS product compounds of the KEC-VGOs.
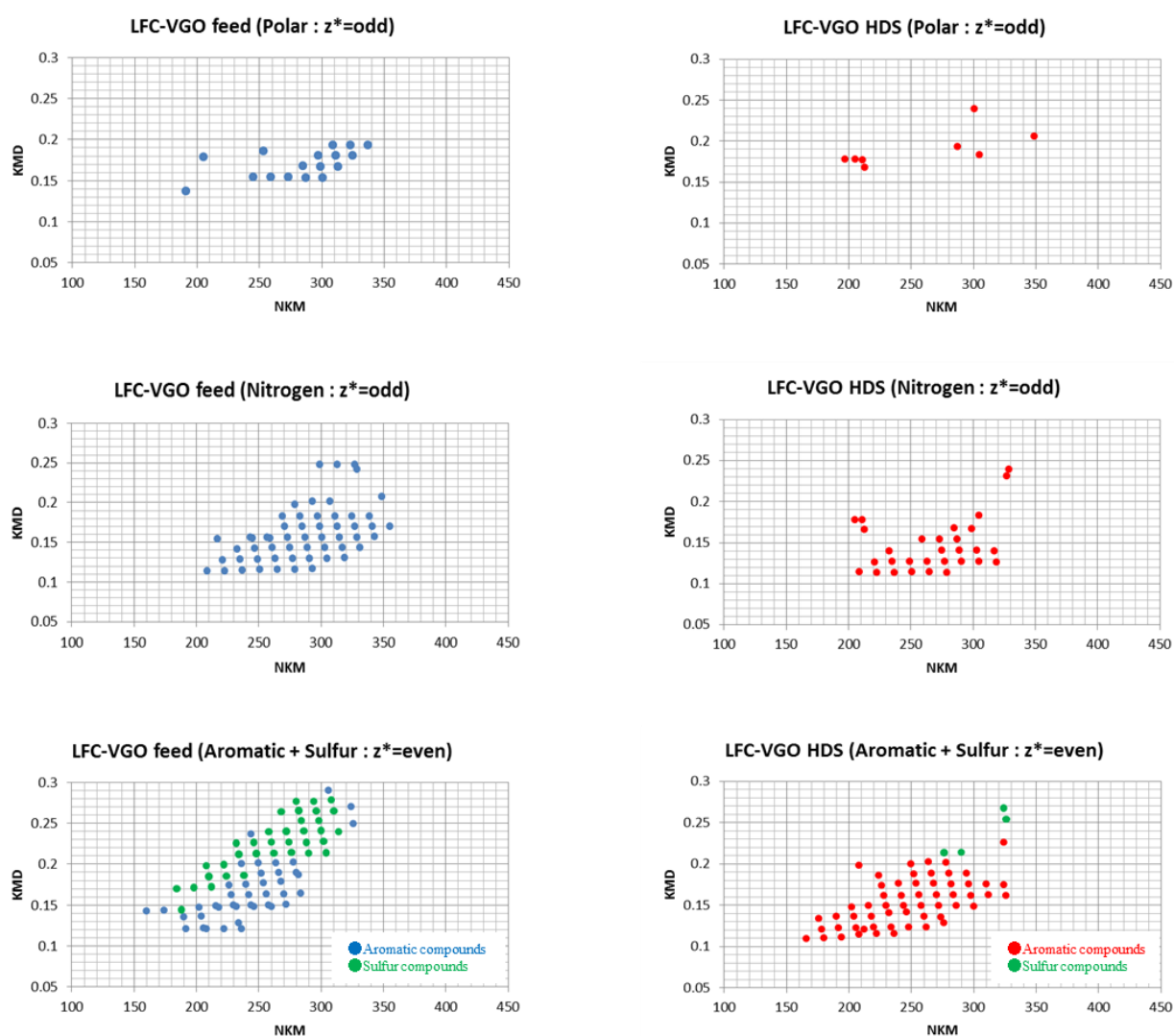

Figure 6. Kendrick plot of each fraction in LFC-VGO feed and HDS product.

3.2.2. Aromatic and Sulfur Fractions in LFC-VGO Feed and HDS Products

Aromatic and sulfur fractions in LFC-VGO showed similar KEC patterns. Sulfur compounds have large KMD values and aromatics have small KMD values, but some compounds were plotted in the low KMD range. In the HDS products, a few benzonaphthothiophenes, chrysenothiophenes and cholanthrenothiophenes were detected. As for the other compounds, octahydronaphthacene, anthracene, tetrahydrobenzoanthracene, pyrene, chrysene, tetrahydropicene and perylene were confirmed to be present (Table 3), similar to the HDS products of KEC-VGO. In both KEC-VGO and LFC-VGO, the number of compounds with large KMD values decreased, while compounds with small KMD values remained after the reaction. This shows that compounds with a high DBE are hydrogenated because they have some benzene rings. Benzene rings have π bonds that are easily converted into σ bonds, so the catalyst interacts with π electrons in the benzene rings and the bonds are cut under high hydrogen pressure. Compounds with abundant benzene rings have many π electrons; thus, these compounds interact with the surface of the catalyst, such that compounds with a high DBE are hydrogenated first. Interestingly, the molecular weight of some compounds in the HDS product is larger than that of certain compounds in the KEC-VGO. It is possible that compounds with a high molecular weight and high DBE cannot be ionized, or that the concentration is quite small. Gel permeation chromatography (GPC) analysis was conducted for the feed and HDS products of aromatic and sulfur fractions in the VGOs. Based on the results of the GPC analysis, the molecular size decreased (Figure 7), so the molecular weight became smaller after the HDS reaction, and some compounds with a high molecular weight and high DBE could not be ionized.
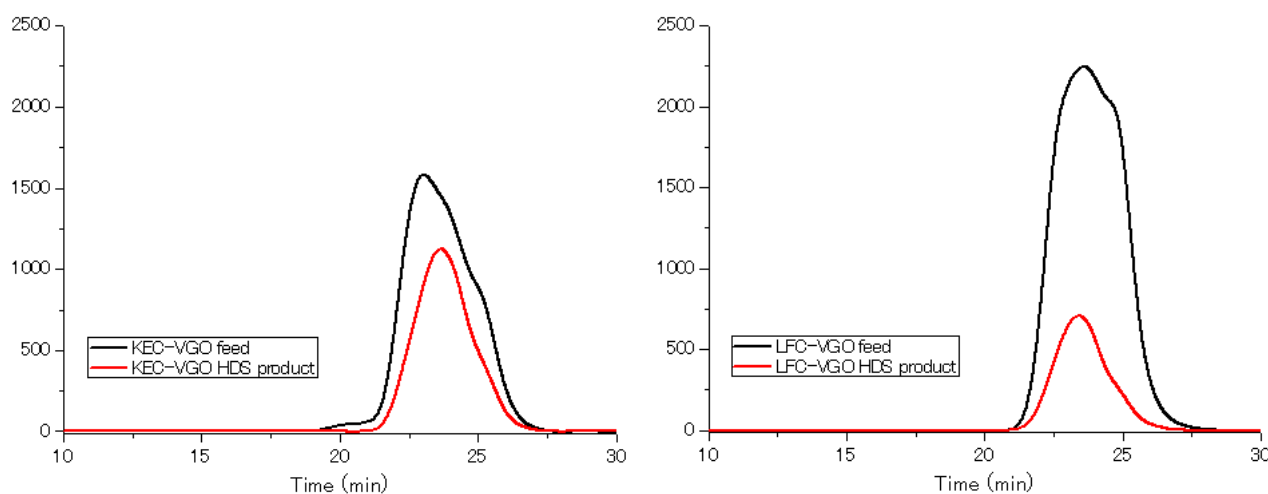

Figure 7. Results of GPC analysis for (**left**) KEC-VGO and (**right**) LFC-VGO. Black line: feed; red line: HDS product.

4. Conclusions

Prior to the application of MALDI-TOF-MS analysis, sample fractionation was performed using liquid chromatography in the presence of packed alumina as a pre-separation procedure. The spectra proved to be more effective in analyzing VGOs, as a greater number of peaks appeared after fractionation than in the non-pre-separated samples. Careful matrix selection is one of the most important aspects of MALDI-TOF/MS. In this work, 4,6-DMDBT was investigated as a standard sample to find the most suitable measurement conditions. TCNQ proved to be the best matrix as it ensured that the ionized compound was in a radical state due to its four cyano groups. In order to obtained high-resolution data, internal standard and external standard methods were evaluated and shown to be effective, as long as standard samples were used, and the mass defect was kept to a minimum. The Kendrick plot is a well-known method for interpreting mass data. The employment of nominal mass series (z^*) is an effective alternative method. Since the difference in KMD between $C_nH_{2n-14}S$ and $C_nH_{2n-20}O$ is only 0.0005 mass units, it is not an easy task to

distinguish these compounds without further refining the data. However, the z* value was different between these compounds; therefore these species can be classified on the basis of this value. Using z* values, compounds of each fraction in the VGOs were apparently classified. In the case of the polar and nitrogen fractions of both VGOs, N_1 species were dominant and a few S_1N_1 species were also present. Compounds in the polar fractions of the KEC-VGO feed had longer alkyl chains compared with those of the LFC-VGO feed, and in the nitrogen fractions, alkyl chains of the KEC-VGO feed were longer than those of the LFC-VGO feed. After the HDS reaction was applied to both VGOs, compounds of a high molecular weight and high DBE were reduced in number. This supports the idea that alkyl chains were cut, and benzene rings were hydrogenated in the presence of hydrogen. Though it was not expected, there was no major difference in the plots of the aromatic and sulfur fractions between the KEC-VGO and LFC-VGO feeds. Sulfur-containing compounds corresponded to high values of KMD in the Kendrick plot, while aromatic compounds corresponded to low values of KMD. After the HDS reaction, almost all sulfur compounds were reduced and aromatic compounds appeared with a low DBE. Although the compounds were hydrogenated, the molecular weight of some species in the HDS product was larger than that of compounds dispersed in the feed. It may be possible that species of a larger molecular weight were present in the VGO, but were hardly detected due to the low concentrations or inappropriate conditions for ionization.

Supplementary Materials: The following supporting information can be downloaded at: https://www.mdpi.com/article/10.3390/molecules29112508/s1.

Author Contributions: Conceptualization, M.U. and K.N.; methodology, J.-I.P.; validation, J.L. and S.-H.Y.; formal analysis, H.Y., K.O. and G.-H.L.; investigation, K.N. and J.-I.P.; resources, Y.-J.K., K.O., S.-H.Y. and J.-I.P.; data curation, M.U.; writing—original draft preparation, M.U.; writing—review and editing, K.N. and J.-I.P.; visualization, G.-H.K.; supervision, K.N. and J.-I.P.; project administration, K.N. and J.-I.P. All authors have read and agreed to the published version of the manuscript.

Institutional Review Board Statement: Not applicable.

Informed Consent Statement: Not applicable.

Data Availability Statement: Data are contained within the article and Supplementary Materials.

Conflicts of Interest: The authors declare no conflict of interest.

References

1. Klein, G.C.; Rodgers, R.P.; Marshall, A.G. Identification of hydrotreatment-resistant heteroatomic species in a crude oil distillation cut by electrospray ionization FT-ICR mass spectrometry. *Fuel* **2006**, *85*, 2071–2080. [CrossRef]
2. Stanford Lateefah, A.; Kim, S.; Rodgers Ryan, P.; Marshall Alan, G. Characterization of Compositional Changes in Vacuum Gas Oil Distillation Cuts by Electrospray Ionization Fourier Transform−Ion Cyclotron Resonance (FT−ICR) Mass Spectrometry. *Energy Fuels* **2006**, *20*, 1664–1673. [CrossRef]
3. Frątczak, J.; de Paz Carmona, H.; Tišler, Z.; Hidalgo Herrador, J.; Gholami, Z. Hydrocracking of Heavy Fischer–Tropsch Wax Distillation Residues and Its Blends with Vacuum Gas Oil Using Phonolite-Based Catalysts. *Molecules* **2021**, *26*, 7172. [CrossRef] [PubMed]
4. Luna, N.; Zelong, L.; Songbai, T. Identification and Characterization if Sulfur Compounds in Straight- Run Diesel Using Comprehensive Two-Dimensional GC Coupled with TOF/MS. *China Pet. Process. Petrochem. Technol.* **2014**, *16*, 10–18.
5. Ishihara, A.; Dumeignil, F.; Lee, J.; Mitsuhashi, K.; Qian, E.W.; Kabe, T. Hydrodesulfurization of sulfur-containing polyaromatic compounds in light gas oil using noble metal catalyst. *Appl. Catal. A: Gen.* **2005**, *289*, 163–173. [CrossRef]
6. Azizi, N.; Ali, S.A.; Alhooshani, K.; Kim, T.; Lee, Y.; Park, J.I.; Miyawaki, K.; Yoon, S.H.; Mochida, I. Hydrotreating of light cycle oil over NiMo and CoMo catalysts with different supports. *Fuel Process. Technol.* **2013**, *109*, 172–178. [CrossRef]
7. Amrani, A.; Deev, A.; Sessions, A.; Tang, Y.; Adkins, J.F.; Hill, R.J.; Moldowan, M.; Wel, Z. The sulfur-isotopic compositions of benzothiophenes and dibenzothiophenes as a proxy for thermochemical sulfate reduction. *Geochim. Cosmochim. Acta* **2012**, *84*, 152–164. [CrossRef]

8. Schade, T.; Andersson, J.T. Speciation of Alkylated Divenzothiophenes in a Deeply Desulfurized Diesel Fuel. *Energy Fuel* **2006**, *20*, 1614–1620. [CrossRef]

9. Schade, T.; Andersson, J.T. Speciation of alkylated dibenzothiophenes through correlation of structure and gas chromatographic retention indexes. *J. Chromatogr. A* **2006**, *1117*, 206–213. [CrossRef]

10. Hughey, C.A.; Hendrickson, C.L.; Rodgers, R.P.; Marshall, A.G. Elemental Composition Analysis of Processed and Unprocessed Diesel Fuel by Electrospray Ionization Fourier Transform Ion Cyclotron Resonance Mass Spectrometry. *Energy Fuel* **2001**, *15*, 1186–1193. [CrossRef]

11. Schaub, T.M.; Rodgers, R.P.; Marshall, A.G. Speciation of Aromatic Compounds in Petroleum Refinery Streams by Continuous by Flow Field Desorption Ionization FT-ICR Mass Spectrometry. *Energy Fuel* **2005**, *19*, 1566–1573. [CrossRef]

12. Xiaobo, C.; Yibin, L.; Jin, W.; Honghong, S.; Chaohe, Y.; Chunyi, L. Characterization of nitrogen compounds in coker gas oil by electrospray ionization Fourier transform ion cyclotron resonance mass spectrometry and Fourier transform infrared spectroscopy. *Appl. Petrochem. Res.* **2014**, *4*, 417–422. [CrossRef]

13. Rodgers, R.P.; Hendrickson, C.L.; Emmett, M.R.; Marshall, A.G. Reading Chemical Fine Print: Resolution and Identification of 3000 Nitrogen-Containing Aromatic Compounds from a Single Electrospray Ionization Fourier Transform Ion Cyclotron Resonance Mass Spectrum of Heavy Petroleum Crude Oil. *Energy Fuel* **2001**, *15*, 492–498.

14. Zhu, X.; Shi, Q.; Zhang, Y.; Pan, N.; Xu, C.; Chung, K.H.; Zhao, S. Characterization of Nitrogen Compounds in Coker Heavy Gas Oil and Its Subfractions by Liquid Chromatographic Separation Followed by Fourier Transform Ion Cyclotron Resonance Mass Spectrometry. *Energy Fuel* **2011**, *25*, 281–287. [CrossRef]

15. Shi, Q.; Xu, C.; Zhao, S.; Chung, K.H.; Zhang, Y.; Gao, W. Characterization of Basic Nitrogen in Coker Gas Oils by Positive-Ion Electrospray Ionization Fourier Transform Ion Cyclotron Resonance Mass Spectrometry. *Energy Fuel* **2010**, *24*, 563–569. [CrossRef]

16. Chen, X.; Shen, B.; Sun, J.; Wang, C.; Shan, H.; Yang, C.; Li, C. Characterization and Comparison of Nitrogen Compounds in Hydrotreated and Untreated Shale Oil by Electrospray Ionization (ESI) Fourier Transform Ion Cyclotron Resonance Mass Spectrometry (FT-ICR MS). *Energy Fuel* **2012**, *26*, 1707–1714. [CrossRef]

17. Li, Z.K.; Wang, G.; Shi, Q.; Xu, C.M.; Gao, J.S. Retardation Effect of Basic Nitrogen Compounds on Hydrocarbons Catalytic Cracking in Coker Gas Oil and Their Structural Identification. *Ind. Eng. Chem. Res.* **2011**, *50*, 4123–4132. [CrossRef]

18. Shi, Q.; Zhao, S.; Xu, Z.; Chung, K.H.; Zhang, Y.; Xu, C. Distribution of Acids and Neutral Nitrogen Compounds in a Chinese Crude Oil and Its Fractions: Characterized by Negative-Ion Electrospray Ionization Fourier Transform Ion Cyclotron Resonance Mass Spectrometry. *Energy Fuel* **2010**, *24*, 4005–4011.

19. Cho, Y.; Kim, Y.H.; Kim, S. Planar Limit-Assisted Structural Interpretation of Saturates Aromatics Resins Asphaltenes Fractionated Crude Oil Compounds Observed by Fourier Transform Ion Cyclotron Resonance Mass Spectrometry. *Anal. Chem.* **2011**, *83*, 6068–6073. [CrossRef]

20. Zhang, Y.; Shi, Q.; Li, A.; Chung, K.H.; Zhao, S.; Xu, C. Partitioning of Crude Oil Acidic Compounds into Subfractions by Extrography and Identification of Isoprenoidyl Phenols and Tocopherols. *Energy Fuel* **2011**, *25*, 5083–5089. [CrossRef]

21. Zhang, T.; Zhang, L.; Zhou, Y.; Wei, Q.; Chung, K.H.; Zhao, S.; Xu, C.; Shi, Q. Transformation of Nitrogen Compounds in Deasphalted Oil Hydrotreating: Characterized by Electrospray Ionization Fourier Transform-Ion Cyclotron Resonance Mass Spectrometry. *Energy Fuel* **2013**, *27*, 2952–2959. [CrossRef]

22. Li, X.; Zhu, J.; Wu, B.; Mao, X. Characterization of Acidic Compounds in Vacuum Gas Oils and Their Dewaxed Oils by Fourier Transform-Ion Cyclotron Resonance Mass Spectrometry. *Energy Fuel* **2012**, *26*, 5646–5654. [CrossRef]

23. Zhang, J.; Shan, H.; Chen, X.; Liu, W.; Yang, C. Synergistic Process for High Nitrogen Content Feedstocks Catalytic Cracking: A Case Study of Controlling the Reactions of Nitrogen Compounds in Situ. *Ind. Eng. Chem. Res.* **2014**, *53*, 5718–5727. [CrossRef]

24. Fu, J.; Klein, G.C.; Smith, D.F.; Kim, S.; Rodgers, R.P.; Hendrickson, C.L.; Marshall, A.G. Comprehensive Compositional Analysis of Hydrotreated and Untreated Nitrogen-Concentrated Fractions from Syncrude Oil by Electron Ionization, Field Desorption Ionization, and Electrospray Ionization Ultrahigh-Resolution FT-ICR Mass Spectrometry. *Energy Fuel* **2006**, *20*, 1235–1241. [CrossRef]

25. Hugheya, C.A.; Rodgersa, R.P.; Marshalla, A.G.; Qianc, K.; Robbinsc, W.K. Identification of acidic NSO compounds in crude oils of different geochemical origins by negative ion electrospray Fourier transform ion cyclotron resonance mass spectrometry. *Org. Geochem.* **2002**, *33*, 743–759. [CrossRef]

26. Dutriez, T.; Courtiade, M.; Ponthus, J.; Thiébaut, D.; Dulot, H.; Hennion, M.C. Complementary of Fourier Transform Ion Cyclotron Resonance Mass Spectrometry and high temperature comprehensive two-dimensional gas chromatography for the characterization of resin fractions from vacuum gas oils. *Fuel* **2012**, *96*, 108–119. [CrossRef]

27. Wiwel, P.; Hinnemann, B.; Vivas, A.H.; Zeuthen, P.; Petersen, B.O.; Duus, J. Ø. Characterization and Identification of the most Refractory Nitrogen Compounds in Hydroprocessed Vacuum Gas Oil. *Ind. Eng. Chem. Res.* **2010**, *49*, 3184–3193. [CrossRef]

28. Thomson, J.S.; Green, J.B.; McWilliams, T.B. Determination of sulfides and thiols in petroleum distillates using solid-phase extraction and derivatization with pentafluorobenzoyl chloride. *Energy Fuels* **1997**, *11*, 909–914. [CrossRef]

29. de Peinder, P.; Visser, T.; Wagemans, R.; Blomberg, J.; Chaabani, H.; Soulimani, F.; Weckhuysen, B.M. Sulfur Speciation of Crude Oils by Partial Least Squares Regression Modeling of Their Infrared Spectra. *Energy Fuels* **2010**, *24*, 557–562. [CrossRef]

30. Dijkmans, T.; Van Geem, K.M.; Djokic, M.R.; Marin, G.B. Combined Comprehensive Two-Dimensional Gas Chromatography Analysis of Polyaromatic Hydrocarbons /Polyaromatic Sulfur-Con-taining Hydrocarbons (PAH/PASH) in Complex Matrices. *Ind. Eng. Chem. Res.* **2014**, *53*, 15436–15446. [CrossRef]

31. Melville, J. Matrix-Assisted Laser Desorption/Ionization(MALDI). *UC Berkeley Coll. Chem. Instrum. Methods Anal. Chem.* **2014**, 1–16.
32. Ibarra, A.; Veloso, A.; Bilbao, J.; Arendes, J.M.; Castano, P. Dual coke deactivation pathways during the catalytic cracking of rawbio-oil and vacuum gasoil in FCC conditions. *Appl. Catal. B Environ.* **2016**, *182*, 336–346. [CrossRef]
33. Panda, S.K.; Andersson, J.T.; Schrader, W. Characterization of supercomplex crude oil mixtures: What is really in there? *Angew. Chem. Int. Ed.* **2009**, *48*, 1788–1791. [CrossRef] [PubMed]
34. Shiraishi, Y.; Hirai, T.; Komasawa, I. Photochemical Desulfurization and Denitrogenation Prodcess for Vacuum Gas Oil Using an Organic Two-Phase Extraction System. *Ind. Eng. Chem. Res.* **2001**, *40*, 293–303. [CrossRef]
35. Yang, J.; Nakabayashi, K.; Miyawaki, J.; Yoon, S.-H. Preparation of isotropic pitch-based carbon fiber using hyper coal through co-carbonation with ethylene bottom oil. *J. Ind. Eng. Chem.* **2016**, *34*, 397–404. [CrossRef]
36. Kendrick, E. A Mass Scale Based on $CH_2 = 14.0000$ for High Resolution Mass Spectrometry of Organic Compounds. *Anal. Chem.* **1963**, *35*, 2146–2154. [CrossRef]